Asian Journal of Chemistry; Vol. 37, No. 6 (2025), 1358-1366

ASIAN JOURNAL OF CHEMISTRY

https://doi.org/10.14233/ajchem.2025.33773

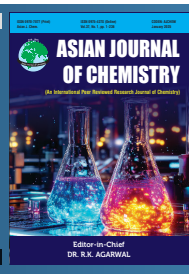

Synthesis, Quantum Chemical, Spectral, Optical, Thermal and Biological Studies on Sulfamethazine Single Crystal

J. Jebamalar Belciya[1,2], R. Anitha[2,*], M. Mohamed Roshan[1], R. Renugadevi[3] and S. Athimoolam[4]

[1]Department of Physics & Research Centre, Sadakathullah Appa College (Autonomous) (Affiliated to Manonmaniam Sundaranar University, Tirunelveli), Tirunelveli-627011, India
[2]Department of Physics & Research Centre, Sarah Tucker College (Autonomous) (Affiliated to Manonmaniam Sundaranar University, Tirunelveli), Tirunelveli-627007, India
[3]Department of Physics, KGiSL Institute of Technology, Coimbatore-641035, India
[4]Department of Physics, Anna University Regional Campus, Tirunelveli-627007, India

*Corresponding author: E-mail: anitha1984r@gmail.com

Received: 13 March 2025; *Accepted*: 1 May 2025; *Published online*: 27 May 2025; AJC-22009

The single crystal of the pharmaceutical drug sulfamethazine has been grown using the slow evaporation method at ambient temperature. The analysis of the single crystal X-ray diffraction (XRD) data indicates that the grown crystal belongs to the monoclinic crystal system. This classification is based on the symmetry and the lattice parameters observed during the single crystal XRD analysis. The optimized geometry of sulfamethazine molecule was determined using two methods *viz*. density functional theory (DFT) and restricted Hartree-Fock (RHF) in the gas phase. Spectral analysis of grown crystal was performed, offering an examination of its vibrational modes and providing the functional groups of the compound. The Mulliken atomic charge distribution was also computed to provide information about the electron density distribution across the molecule, highlighting the nature of charge transfer between atoms. Sulfamethazine crystals demonstrate high transmittance in the 190-1100 nm range, as observed in the UV-visible spectrum. The thermal behavior of the studied compound was examined through TGA/DTA analysis and revealed that the crystal maintains thermal stability up to 210 ºC. The sulfamethazine aslo exhibit significant antibacterial effects against bacterial species such as *Escherichia coli* and *Staphylococcus aureus*, highlighting their potential as an effective antimicrobial agent.

Keywords: Sulfamethazine, Slow evaporation, Computational studies, DFT, Thermal study, Antibacterial activity.

INTRODUCTION

Sulfamethazine, also known as sulfadimidine, is a antibiotic commonly used in veterinary and agriculture to treat bacterial infections in animals. Sulfamethazine works by inhibiting bacterial dihydropteroate synthase, an enzyme crucial for the production of folic acid, thereby preventing the growth and reproduction of bacteria [1,2]. It is also a key component of the triple sulfa drugs [3]. Sulfamethazine compounds are widely used as a result of their antibacterial characteristics and the single crystal X-ray structures of the studied compounds have been reported [4,5]. Many sulfonamide drugs possess the ability to form solvates [6] and show the polymorphism [7,8]. The ability of sulfamethazine to form solvates when combined with methanol, pyridine and 3-methylpyridine [9,10]. Moreover, the crystal structure of pure solid sulfamethazine has been previously reported [11]. The impact of impurities with similar structural properties on the grinding-induced reduction of sulfamethazine crystals has also been examined [12].

Quantum chemical computations have garnered significant interest in various fields of study in recent years. Density functional theory (DFT) techniques are becoming increasingly popular due to their effectiveness in understanding a wide range of complex phenomena in biology and chemistry [13-15]. Recent years have seen a scarcity of work employing DFT to conceptually examine sulfamethazine molecules [16-22]. However, minimal information is available regarding the chemical structure, modes of vibration and global descriptive parameters of the title compound in relation to various theories and basis sets. A deeper comprehension of the electrical structure and

chemical characteristics of sulfamethazine molecule is crucial for their use in different applications. The present study utilizes density functional theory (DFT) and the restricted Hartree-Fock (RHF) methods to compute the optimized molecular geometries, frontier molecular orbitals, Mulliken atomic charges and vibrational spectra of sulfamethazine molecules at the RB3LYP level of theory, using the 6-311++G(d, p) basis set. Furthermore, the UV-visible analysis and thermal studies were also studied on the title compound. The primary goal of this study is to analyze antibacterial activity of sulfamethazine due to its pharmaceutical applications.

EXPERIMENTAL

Crystal growth: Sulfamethazine compound was grown by dissolving the compound in methanol under constant magnetic stirring and then allowed to undergo the slow evaporation process under controlled conditions to facilitate crystal growth. After 4 days, the solution gradually evaporated, leading to the formation of a high-quality single crystal. Fig. 1 shows the photograph of single crystal of sulfamethazine.

Fig. 1. Photograph of sulfamethazine single crystal

Characterization: Using Bruker SMART APEX CCD single crystal X-ray diffractometer (graphite-monochromated, Mo*K*α = 0.71073 Å), the grown sulfamethazine crystal has been subjected to single crystal X-ray diffraction (XRD) analysis [23]. The Bruker IF S66v FT-IR spectrometer was utilized to record the FTIR utilizing the KBr pellet technique, covering a range of 4000 cm^{-1} to 400 cm^{-1}. The FT-Raman spectrum was measured between 50 and 4000 cm^{-1} using a Briker-RFS27 FT-Raman spectrometer. The UV-Vis transmission spectrum was recorded between 190 and 1100 nm using a Perkin-Elmer Lambda 35 UV-Vis spectrophotometer. The SDT Q 650 thermal analyzer was used to analyze the crystalline substance between 20 to 800 ºC.

Computational details: The optimized molecular geometry and atomic charge distribution of sulfamethazine molecule were calculated using quantum chemical computations based on density functional theory (DFT) and restricted Hartree-Fock (RHF) methods. The quantum chemical calculations were performed using Gaussian 09W software with the 6-311++G (d, p) basis set in the gas phase. The Lee-Yang-Parr correlation functional (RB3LYP), a hybrid functional that integrates Becke's three-parameter exchange functional, was employed for the DFT calculations [24,25]. The optimization of the molecular geometry was carried out using both DFT and RHF methods to compare the geometrical parameters. Mulliken charges were calculated using the same theoretical model. The theoretical spectroscopic properties of sulfamethazine were also studied using both the DFT and RHF methods in the gas phase. These studies focused on optimizing the molecular geometry, understanding electron density distribution and investigating vibrational frequencies, energy gaps and molecular orbitals (HOMO-LUMO analysis).

RESULTS AND DISCUSSION

Single crystal X-ray studies: The lattice parameters values of the grown sulfamethazine single crystal were successfully determined through single crystal X-ray diffraction analysis. A monoclinic crystal system with space group $P2_1/c$ forms within the grown crystal of sulfamethazine. Table-1 illustrates the cell parameters which have been obtained.

TABLE-1
CRYSTALLOGRAPHIC DATA FOR SULFAMETHAZINE CRYSTAL

Empirical formula	$C_{12}H_{14}N_4O_2S$
Formula weight	278.33 g mol^{-1}
Temperature	293(2) K
Wavelength	0.71073 Å
Crystal system	Monoclinic
Space group	$P2_1/c$
Unit cell dimensions	a = 9.3146(5) Å
	b = 18.9685(10) Å, β =99.04(3)°
	c = 7.4178 (3) Å
Volume	1294 (2) A^3

Optimized molecular geometry: The theoretical studies employing restricted Hartree-Fock (RHF) and density functional theory (DFT) techniques were conducted to compute the optimized molecular geometry. The DFT/RB3LYP and RHF method were used to identify the optimized geometrical parameters for the sulfamethazine molecule using the 6-311++ G (d, p) basis set. Fig. 2 displays the optimized structure of sulfamethazine compound with the numbered atoms. Table-2 presents the geometric properties of dihedral angles, bond lengths and bond angles. The sulfamethazine compound observed between the sulfur and nitrogen atoms in the sulfonamide group (-SO_2NH). For sulfamethazine molecule, the S8-N11 bonds length to 1.711 Å in DFT and 1.6325 Å in RHF methods. In present case, the sulfonamide group was obtained in the bond angle of O9-S8-O10 in the range about 121.3981° in DFT and RHF method are 117.9581° respectively. In computational method, the optimized molecular geometry studies of sulfamethazine single crystals to provide a detailed understanding of the molecular structure and interactions.

Vibrational studies: Using a solid phase Bruker IF S66v spectrometer, the experimental FT-IR spectra of the sulfamethazine molecule were obtained in the 4000 to 400 cm^{-1} range. Having 33 atoms, the sulfamethazine molecule exhibits 93 normal modes of vibration. The characteristic vibrations of

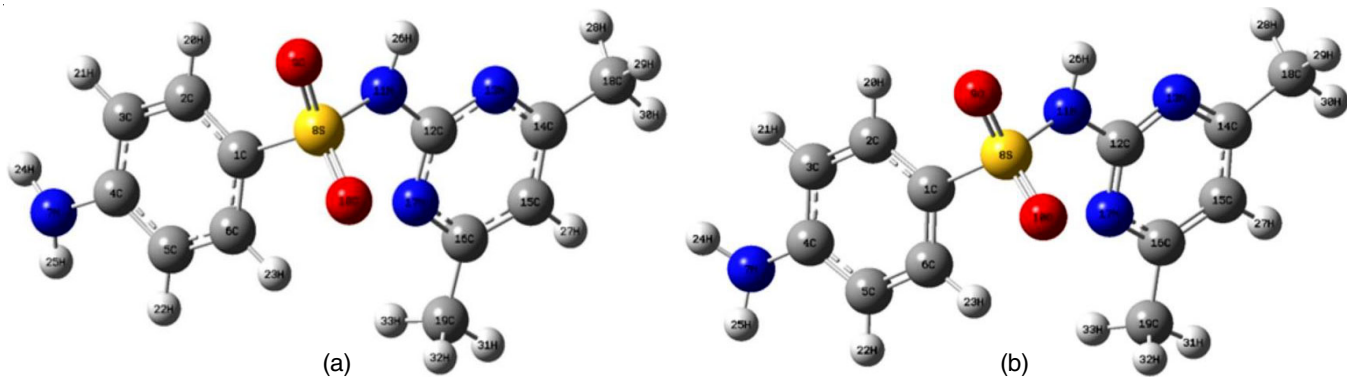

Fig. 2. View of title compound showing the optimized geometry structure at DFT/RB3LYP and RHF method with 6-311++G(d,p) basis set

TABLE-2
OPTIMIZED GEOMETRICAL PARAMETERS OF THE TITLE COMPOUND

Bond length (Å)			Bond angle (º)			Dihedral angles (º)		
Parameters	RB3LYP/6-311++G (d,p)	RHF/6-311++G(d,p)	Parameters	RB3LYP/6-311++G (d,p)	RHF/6-311++G(d,p)	Parameters	RB3LYP/6-311++G (d,p)	RHF/6-311++G(d,p)
C1-C2	1.3956	1.3615	C2-C1-C6	120.7041	121.7292	C6-C1-C2-H20	178.6976	177.1087
C1-C6	1.3942	1.3988	C2-C1-S8	119.2942	121.3976	S8-C1-C2-C3	-179.305	-177.62
C1-S8	1.7787	1.7654	C6-C1-S8	119.9935	116.6275	S8-C1-C2-H20	-0.2611	2.9958
C2-C3	1.3856	1.3816	C1-C2-C3	119.6423	119.903	C2-C1-C6-C5	0.1248	1.9397
C2-H20	1.0828	0.9377	C1-C2-H20	119.9542	120.726	C2-C1-C6-H23	-179.929	-173.854
C3-C4	1.4069	1.3979	C3-C2-H20	120.3965	119.3682	S8-C1-C6-C5	179.0762	176.3192
C3-H21	1.0848	0.9695	C2-C3-C4	120.5786	119.5951	S8-C1-C6-H23	-0.9779	0.5252
C4-C5	1.4062	1.3726	C4-C3-H21	119.6567	128.8503	C2-C1-S8-O9	23.8258	55.625
C4-N7	1.3844	1.3581	C3-C4-C5	118.8303	120.1099	C2-C1-S8-O10	157.9869	-174.653
C5-C6	1.3861	1.396	C5-C4-N7	120.6001	119.5386	C6-C1-S8-O10	-20.9794	10.9472
C5-H22	1.0849	1.0069	C4-C5-C6	120.7121	120.6984	C1-C2-C3-H21	179.2767	-178.411
C6-H23	1.0814	1.0045	C1-C6-C5	119.5311	117.8765	H20-C2-C3-C4	-178.841	-178.155
N7-H24	1.0079	1.178	C1-C6-H23	119.5821	122.4764	H20-C2-C3-H21	0.2374	0.9818
N7-H25	1.0079	1.0075	C5-C6-H23	120.8868	119.5147	N11-C12-N13-C14	-178.454	-172.521
S8-O9	1.4622	1.4304	C4-N7-H24	117.4631	146.9723	N17-C12-N13-C14	-0.291	0.3475
S8-O10	1.4555	1.4256	O9-S8-O10	121.3981	117.9581	N11-C12-N17-C16	179.3903	172.9141
S8-N11	1.711	1.6325	O9-S8-N11	101.4816	102.8946	C12-N13-C14-C18	179.6138	-177.675
N11-C12	1.3906	1.4115	O10-S8-N11	109.9478	110.6641	N13-C14-C15-C16	0.7138	5.119
N11-H26	1.0132	1.0688	S8-N11-C12	126.9751	125.9824			
C12-N13	1.3376	1.3429	N11-C12-N17	118.1242	118.0225			
C12-N17	1.3316	1.2941	N13-C12-N17	127.3511	129.4804			
N13-C14	1.337	1.3546	C15-C14-C18	122.3003	123.878			
C14-C18	1.5028	1.4949	C14-C15-C16	117.8648	121.4748			
C15-C16	1.3946	1.355	C14-C15-H27	121.0229	114.5278			
C15-H27	1.0823	0.9703						
C16-C19	1.5028	1.4866						
C19-H33	1.0933	0.8894						
C14-C15	1.3968	1.3664						

the C–H, C–N, N–H, SO_2 and CH_3 groups were formed as the basis for the FTIR and FT-Raman investigations. The computed wavenumbers from the DFT and RHF calculations are consistent with the experimental values. Theoretical calculations for gas space were carried out, in contrast to the experimental values that were obtained using solid phase. In Figs. 3 and 4, the observed FTIR and FT-Raman values are compared between the computational and experimental results. Table-3 clearly shows that the titled molecule exhibits different types of vibrations: torsion (T), bending (β) and stretching (ν). Scissoring (sci), wagging (wag) and out-of-plane bending (out) are the characteristics of the bending vibrations.

N-H vibrations: The stretching vibrations of the NH group, both asymmetric and symmetric, are expected to occur in the 3500-3300 cm^{-1} region [26]. The strength of hydrogen bonding interaction determines the vibrational frequencies of N-H stretching, bending and deformation bands. In sulfamethazine molecule, the N-H asymmetric stretching vibrations of IR spectrum was observed in the 3905-3691 cm^{-1} region in DFT/RHF studies and the same vibrations had occurred at 3853 cm^{-1}in the experimental spectra. The wavenumbers for N-H symmetric stretching vibrations were computed at 3587 cm^{-1} using the DFT method and at 3832 cm^{-1} using the RHF method, both with the 6-311++G (d, p) basis set. These vibrations were absent in

TABLE-3
EXPERIMENTAL AND CALCULATED (DFT/RHF) VIBRATIONAL ASSIGNMENTS OF SULFAMETHAZINE COMPOUND

Experimental		RB3LYP/6-311++G(d,p)			RHF/6-311++G(d,p)			Assignments
FT- IR (cm^{-1})	FT-Raman (cm^{-1})	Wavelength	FT-IR (cm^{-1})	FT-Raman (cm^{-1})	Wavelength	FT- IR (cm^{-1})	FT-Raman (cm^{-1})	
3853.39(w)		3691.54	24.2324	61.6454	3905.46	27.9639	52.9267	N-H asymmetric stretching
		3587.38	44.6674	286.3336	3832.01	119.5219	64.5768	N-H symmetric stretching
3441.37(m)		3584.84	90.7900	85.0916	3801.72	52.8602	189.1693	N-H symmetric stretching
3341.14(m)		3219.58	1.6930	53.9082	3385.51	0.8831	52.3426	C-H stretching vibration
3239.15(m)		3201.95	1.9791	75.8394	3365.34	4.4514	91.9415	C-H stretching vibration
		3195.04	6.8812	123.5311	3363.92	1.6140	70.4071	C-H stretching vibration
		3166.39	14.5958	125.0828	3327.57	13.9253	92.1127	C-H stretching vibration
		3165.26	11.7344	85.8531	3326.12	13.2151	76.8831	C-H stretching vibration
		3120.61	18.8761	75.4514	3262.43	26.9393	71.1817	C-H stretching vibration
		3119.84	15.5301	49.3421	3261.78	20.6156	44.6985	C-H stretching vibration
3095.62(w)		3095.44	7.3838	83.2435	3246.34	11.8758	70.4153	C-H stretching vibration
		3093.63	6.3895	65.1616	3244.44	9.9332	59.3745	C-H stretching vibration
3060.85(w)	3069.52(w)	3038.20	11.2391	301.0150	3182.73	13.8841	231.4777	CH_3 stretching vibration
		3036.70	10.3828	162.3970	3181.22	13.6817	124.6491	CH_3 stretching vibration
1772.05(w)		1663.38	207.7776	40.0836	1810.26	201.9691	39.2007	NH_2 scissoring vibration
1641.04(m)	1638.21(w)	1636.03	105.8224	67.7882	1792.75	417.3324	2.6011	N-H bending vibration
		1621.34	255.9776	5.8596	1774.87	132.3832	75.1294	C-C stretching vibration
		1613.07	16.2335	1.1784	1760.07	599.1197	36.1174	C-C stretching vibration
1595.83(s)	1593.70(s)	1597.03	377.0513	48.7028	1755.86	16.7793	5.4375	C-N stretching vibration
		1529.30	57.5452	6.6739	1659.85	77.9802	1.1717	C-H bending vibration
1505.32(w)		1500.53	30.2527	2.5378	1653.75	141.7863	6.2797	C-N stretching vibration
		1488.87	174.0101	7.8988	1608.12	270.8599	5.0688	CH_2 bending vibration
		1483.02	66.3244	4.4346	1604.16	59.0028	8.9498	CH_2 bending vibration
		1477.20	12.9340	8.6413	1595.21	12.9723	9.7095	CH_3 bending vibration
1476.14(w)		1475.90	4.4703	7.3287	1594.63	2.2129	6.1998	CH_2 bending vibration
		1462.55	20.4236	1.1945	1591.63	207.6742	10.9479	C-C stretching vibration
1433.69(m)		1452.67	326.0597	33.7589	1575.17	11.1407	0.7288	C-N stretching vibration
		1410.92	66.2881	23.8834	1541.80	17.0056	12.6679	CH_3 bending vibration
		1407.62	18.7961	2.4033	1529.84	7.9847	0.3604	CH_2 bending vibration
1383.79(m)		1367.96	58.7929	9.0589	1483.50	86.6204	2.7413	C-C stretching vibration
		1360.49	9.0571	3.9578	1467.91	36.3514	7.4957	C-C stretching vibration
	1342.81(w)	1341.83	49.6925	8.6634	1452.59	2.0085	0.3392	SO_2asymmetric stretching
		1330.83	0.5265	0.7752	1435.40	161.9919	4.3515	C-C stretching vibration
1303.29(m)		1317.33	109.4260	9.6100	1396.29	89.5284	14.8063	C-N stretching vibration
		1294.50	102.4746	8.3133	1330.38	0.4061	2.5727	SO_2 asymmetric stretching
		1255.02	10.9813	1.6279	1297.16	8.9588	1.1545	C-N stretching vibration
		1205.56	19.3696	1.7220	1294.87	7.8131	3.3066	C-C stretching vibration
1189.84(s)		1194.58	7.6376	2.3233	1255.72	52.7095	2.3926	C-C stretching vibration
1143.93(w)	1143.42(w)	1151.14	9.3857	0.3994	1246.40	374.4634	49.4327	C-C stretching vibration
		1125.68	272.4843	98.3543	1203.63	7.8519	0.3158	S-C stretching vibration
1085.36(w)	1090.71(m)	1097.36	18.1504	2.4357	1191.01	3.2379	5.1105	C-N stretching vibration
		1073.23	134.3672	5.2037	1180.71	178.7437	8.4947	C-C stretching vibration
		1069.25	5.0530	1.0017	1159.22	0.1486	0.1290	C-C stretching vibration
		1060.40	0.0784	0.3289	1158.31	1.2675	0.3077	C-H bending vibration
		1054.97	7.1214	0.0349	1155.42	9.3250	0.2231	CH_2 bending vibration
		1038.06	2.5073	1.9174	1112.67	29.7167	4.8278	CH_2 bending vibration
		1021.00	6.1589	1.8415	1100.64	0.1228	0.4726	C-H bending vibration
1004.18(w)	997.29(m)	1012.38	11.9468	41.7494	1096.09	0.5691	13.2787	C-N stretching vibration
		979.24	16.7951	1.3750	1095.01	14.6921	20.2197	C-C stretching vibration
		975.94	0.0477	0.0787	1075.85	0.2417	0.0601	C-H bending vibration
		972.08	37.7379	0.3348	1063.60	53.3016	0.2063	C-N bending vibration
969.58(w)		960.00	0.1813	0.0805	1037.88	16.0166	1.1883	C-H bending vibration
870.35(w)		845.53	12.4126	0.7587	950.73	223.8848	3.4739	C-H stretching vibration
	841.72(m)	843.18	56.0109	14.4412	926.94	53.5839	1.0850	C-C stretching vibration
		833.35	86.6533	1.5222	915.08	23.7314	1.0283	C-N stretching vibration
	825.01(m)	823.23	72.5776	28.6202	907.99	0.4168	0.4502	S-N stretching vibration
		817.32	1.1069	0.6278	902.85	52.4723	2.8165	C-H bending vibration
787.39(m)		804.39	131.4318	21.3368	892.24	5.6218	35.8478	S-N Stretching vibration
		728.06	23.6691	1.2149	800.36	27.4849	1.2166	C-C stretching vibration
		720.68	1.5096	0.2032	788.15	0.9196	1.6984	C-N stretching vibration
		665.18	75.2953	4.0953	738.07	115.1373	1.9360	SO_2 bending vibration
		655.12	4.7736	1.4089	718.43	5.3023	1.1878	C-N bending vibration

631.00(w)	636.41(w)	647.16	0.2768	5.0129	693.19	0.3893	5.2477	C-C bending vibration
580.95(m)	578.58(w)	574.59	117.2284	15.2932	644.82	192.7956	5.1709	C-N stretching vibration
		564.60	2.4732	2.0984	623.28	0.0439	2.3705	C-C bending vibration
		560.25	53.1183	6.9477	614.39	35.2417	1.5215	C-N bending vibration
		544.14	9.6233	2.2206	599.11	17.9275	14.2738	C-N bending vibration
532.79(m)	536.03(w)	535.99	87.0084	1.0575	588.11	191.5702	4.1199	SO_2 bending vibration
		514.82	15.2989	2.8115	583.29	93.9674	2.9477	C-N stretching vibration
		499.46	43.4251	5.1034	540.29	174.2431	10.1514	C-N bending vibration
458.39(w)		452.18	55.0803	1.6572	524.21	42.4323	1.4519	C-S bending vibration
	437.55(w)	439.12	327.0461	7.3056	495.67	8.8524	0.6469	C-N bending vibration
		426.98	31.8776	2.9822	469.12	5.5309	1.2541	C-N bending vibration
		418.51	1.6266	0.1600	456.00	0.7137	0.1372	C-C stretching vibration
		364.07	2.2702	0.8422	402.23	7.4517	0.5777	C-N bending vibration
		349.06	24.2416	1.7520	392.98	4.6543	1.3431	C-N bending vibration
	338.87(w)	344.03	13.9347	0.8812	346.64	2.7910	1.4832	Lattice vibrations
		311.16	3.8414	1.7741	334.25	18.4035	0.2499	Lattice vibrations
		294.77	6.0397	2.8790	330.06	1.8291	3.4068	Lattice vibrations
	267.87(w)	270.21	8.2593	4.1861	297.35	4.4101	3.1111	Lattice vibrations
		257.78	2.6383	3.3176	280.38	0.3359	1.1025	Lattice vibrations
		225.13	1.5385	0.2894	248.46	2.0244	0.5067	Lattice vibrations
	202.91(w)	203.76	1.6571	1.6354	230.04	0.9046	1.1171	Lattice vibrations
	173.25(m)	175.45	0.0144	1.4490	196.62	0.1761	1.1465	Lattice vibrations
		163.96	0.5427	0.7216	184.87	1.8717	0.4594	Lattice vibrations
		161.50	0.8849	0.6781	177.03	4.1269	0.4883	Lattice vibrations
		97.55	0.2247	0.5106	106.09	1.5677	1.4635	Lattice vibrations
		93.02	1.9998	1.7365	101.51	0.5861	0.1782	Lattice vibrations
	81.38(m)	78.90	0.7894	1.9725	89.10	0.3811	1.0414	Lattice vibrations
		72.03	0.1009	0.3987	75.92	0.2139	0.1243	Lattice vibrations
		41.11	0.2686	4.7302	47.75	1.1709	3.9360	Lattice vibrations
		25.77	0.8856	2.5003	29.86	0.2417	2.3193	Lattice vibrations
		22.93	1.0145	6.7700	23.67	1.4770	4.1215	Lattice vibrations

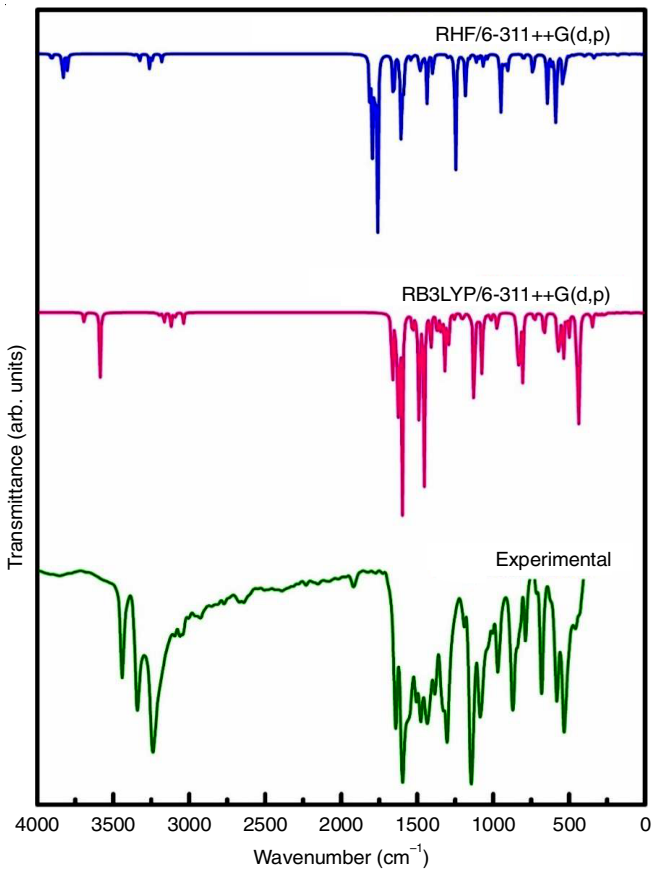

Fig. 3. Calculated and experimental FT-IR spectra of sulfamethazine molecule

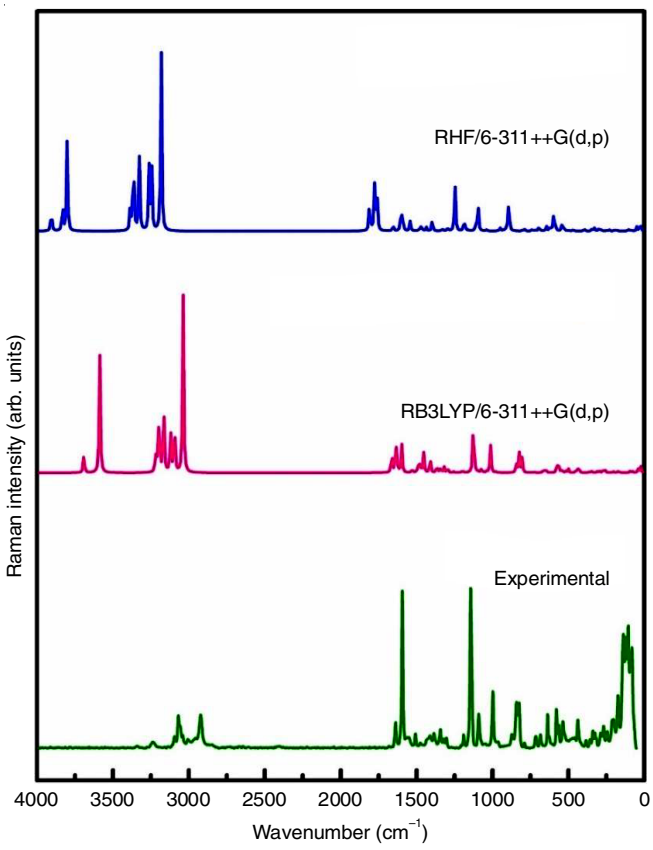

Fig. 4. Calculated and experimental FT-Raman spectra of sulfamethazine molecule

the experimental spectra. The experimentally IR and Raman spectrum determined N-H bending vibration can be found in the region 1641 and 1638 cm^{-1}. The same vibrations were observed in the range of 1636 and 1792 cm^{-1} by DFT/RB3LYP level and RHF method. These experimental results show an excellent correlation with theoretical investigations.

C-H, CH_2, CH_3 vibrations: The symmetric stretching, asymmetric stretching and CH_2 scissoring, as well as CH_2 rocking, are considered in-plane vibrations, whereas CH_2 wagging and CH_2 twisting modes of the CH_2 group are classified as out-of-plane vibrations. These six fundamental vibrations are displayed in the methoxy group frequencies. In the range of 3100-3000 cm^{-1}, which is the characteristic region for rapid identification of C–H stretching vibrations, the aromatic structures exhibit the presence of these vibrations [27,28]. Experimental observations of C-H stretching vibrations had occurred at 3341 and 3239 cm^{-1} in the IR spectra and the FT-Raman spectra was absent for the title molecule. The same vibrations were assigned to theoretically predicted wavenumbers at 3219, 3201, 3195 cm^{-1} and 3385, 3365, 3363 cm^{-1} by the DFT/RB3LYP and RHF methods. The usual expected range for the C-H in-plane bending vibration is 1300-1000 cm^{-1} and these vibrations are excellent for characterization [29]. In present study, C-H in plane bending vibrations were assigned by the computed wavenumbers in the range of 1529 cm^{-1} in DFT and 1659 cm^{-1} in RHF method. The same vibrations are not observed in the experimental spectra. The C-H out-of-plane bending vibrations have normally occurred in the 1100–675 cm^{-1} region [30]. The FT-IR spectra of this work recorded the out-of-plane bending vibrations were computed at 1156-1060 cm^{-1} corresponding to DFT/B3LYP and RHF studies. The CH_2 bending vibrations were computed at 1475 cm^{-1} in DFT and 1594 cm^{-1} in RHF method. The same vibrations were observed in the FT-IR spectra at 1476 cm^{-1} and the Raman spectra was absent in the experimental studies. In theoretical values of DFT and RHF studies, the CH_3 bending vibrations had occurred in the range of 1477 and 1595 cm^{-1}. The experimental spectra were not observed in the same vibrations.

SO_2, S-N vibrations: The asymmetric SO_2 stretching vibrations generally occurred in the 1330-1295 cm^{-1} region [31]. In studied compound, the computed wavenumbers at 1452-1341 cm^{-1} by DFT/RHF method. The experimental IR spectrum was observed at 1342 cm^{-1} and the same vibrations were absent in the Raman spectra. While the SO_2 wagging vibration at 500 ± 55 cm^{-1} and the SO_2 scissoring vibration at 560 ± 40 cm^{-1} are partially overlap, the two vibrations occur separately [32]. The SO_2 bending vibrations had appeared in the 535 cm^{-1} in DFT/RB3LYP and 588 cm^{-1} in RHF method. The FT-IR and FT-Raman spectra show that the same vibrations have occurred at 532 and 536 cm^{-1}, respectively. There is a strong agreement between the calculated wavenumbers and the experimental results for identifying SO_2 bending vibrations. In the S-N stretching vibrations, theoretically occurred at 823 and 907 cm^{-1} in the RB3LYP and RHF methods for sulfamethazine. The IR spectrum shows no vibrations at all, with a medium peak found at 825 cm^{-1} in the Raman spectra.

C-C, C-N vibrations: The existence of a C-C vibration in the 1650–650 cm^{-1} region allows the presence of an aromatic ring easily identifiable [33]. The C-C stretching vibrations are theoretically observed at 1621 cm^{-1} using the DFT/RB3LYP method and at 1774 cm^{-1} using the RHF technique. The same vibrations have not occurred in the experimental spectra. The C-C stretching vibrations can be obtained experimentally in 1383 cm^{-1} in IR spectrum and they are computed at a range of 1367/1483 cm^{-1} by DFT/RHF method. The 1685-1580 cm^{-1} region is associated with the medium stretching vibrations of the C–N bond in the pyridinium molecule [34,35]. The Raman spectrum's band at 1593 cm^{-1} and the medium strong peak vibration of IR spectra at 1595 cm^{-1} in the title molecule both show good correlation with theoretical calculations at 1755 and 1597 cm^{-1} in the RHF and DFT/RB3LYP levels, respectively. In both DFT and RHF, the C-N bending vibration had occurred at 972 cm^{-1} and 1063 cm^{-1}, respectively. This vibration was absent in the experimental studies.

Frontier molecular orbital (FMO) analysis: The sulfamethazine compound was subjected to a frontier molecular orbitals (FMO) investigation utilizing the basis set RB3LYP/RHF with 6-311++G(d, p). Fig. 5 displays the graphic representation of the energy difference for sulfamethazine molecule. Using DFT and RHF methods, the energy gap between the HOMO and LUMO orbits was found to be 3.743 eV and 7.8316 eV, respectively. The eventual charge transfer interaction within the molecule is explained by the energy gap, an analytical parameter used to determine the electrical transport properties of the molecules. For sulfamethazine, the softness values obtained are 0.9357 eV and 2.3761 eV using DFT and RHF methods, respectively.

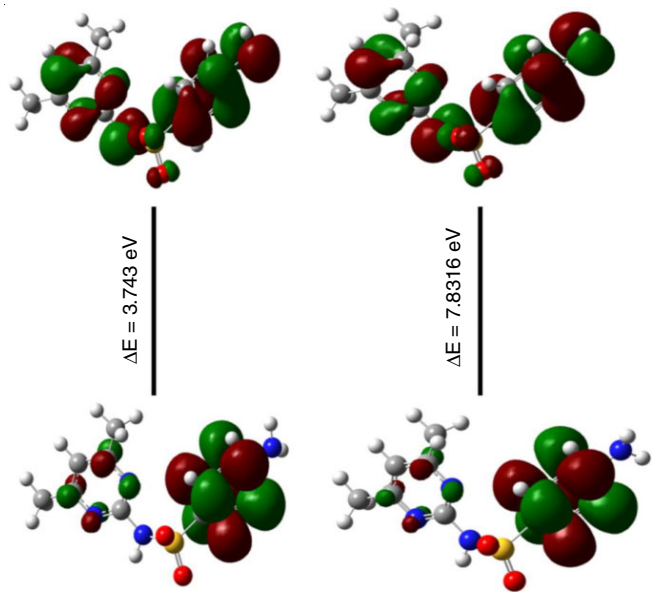

Fig. 5. Frontier molecular orbital of sulfamethazine single crystal

The corresponding hardness values are obtained in 1.8715 eV (DFT) and 4.7522 eV (RHF). The comparative analysis of these parameters highlights the potential for specific pharmaceutical applications of the compound, as it balances stability and reactivity, essential for drug design and activity. Table-4 presents the results of calculations done at the same level for the HOMO and LUMO energies, energy gap (ΔE), ionization

TABLE-4
CALCULATED HOMO-LUMO ENERGY
VALUES OF SULFAMETHAZINE COMPOUND

Quantum description	RB3LYP/6-311++G (d, p)	RHF/6-311++G (d, p)
E_{HOMO} (eV)	-8.3112	-8.6680
E_{LUMO} (eV)	-4.5682	0.8364
Energy gap, ΔE (eV)	3.743	7.8316
Softness (eV)	0.9357	2.3761
Chemical potential, μ (eV)	-6.4397	-3.9158
Electronegativity, χ (eV)	6.4397	3.9158
Hardness, η (eV)	1.8715	4.7522
Electrophilic index, ω (eV)	11.0792	1.6133

potential (I), electron affinity (A), chemical hardness (η), chemical potential (μ), chemical softness (S) and electrophilicity index (ω) of sulfamethazine.

Mulliken charge analysis: The charge distribution in a molecular system can be used to obtain measurements of the dipole moment, polarizability and chemical reactivity. Table-5 presents the Mulliken atomic charges for the sulfamethazine compound, while Fig. 6 illustrates the corresponding data which was calculated using 6-311++G (d, p) basis set and DFT/RB3LYP and RHF methods. In this structure, carbon atoms carry both positive and negative charges. The result reveals that every hydrogen atom has a positive charge. Sulfamethazine is a sulfonamide antibiotic containing a sulfonyl group (-SO_2-) attached to an amine group (-NH_2) and a heterocyclic ring (pyrimidine). These studies have shown that DFT-based Mulliken charges are more accurate in reflecting the chemical nature of the molecule, particularly in regions involving delocalized electrons, such as the aromatic pyrimidine ring in sulfamethazine.The molecular structure and charge distribution play a significant role in understanding its reactivity, binding to biological targets and pharmacological properties.

Optical studies: The optical properties of a grown crystal sample were studied in the wavelength range of 190-900 nm. Figure 7 illustrates the transmittance and absorbance spectra acquired for the 0.88 mm thick optically polished single crystal. The crystals show a good transmittance percentage in the 260–1100 nm range, which has a cut-off wavelength of 262 nm. The material that has the lower cut off wavelength was found in the ultraviolet spectrum, making it suitable for use in medicinal applications. Most dris appear clear to the naked eye because they do not absorb light within the visible spectrum; however, their chemical structure may cause them to absorb light in the UV range [36]. The band gap of the studied crystal was 4.74 eV in accordance with the Tauc's plot relation shown in Fig. 8.

In the sulfamethazine single crystal with an optical band gap energy of 4.74 eV, this suggests that the material is a wide-band-gap semiconductor or insulator. Materials with such a large band gap typically do not absorb visible light but may absorb in the UV range. This band gap helps understand how stable the material is under UV light, which is critical for ensuring the efficacy and safety of the drug over time. As a result, the data obtained showed the grown crystal's excellent optical characteristics, especially high optical transmittance observed at 90% in the visible region. Thus, the results obtained led to the conclusion that sulfamethazine crystal can be applied for various purposes in the pharmaceutical and drug industries.

TABLE-5
MULLIKEN ATOMIC CHARGE DISTRIBUTION OF SULFAMETHAZINE MOLECULE

Atom label	DFT/RB3LYP	RHF/6-311++G(d,p)	Atom label	DFT/RB3LYP	RHF/6-311++G(d,p)	Atom label	DFT/RB3LYP	RHF/6-311++G(d,p)
C1	-0.00163	-0.34268	C12	-0.29105	-0.1004	H23	0.233126	0.2874
C2	-0.12285	-0.08914	N13	-0.00972	-0.06912	H24	0.246596	0.266932
C3	-0.2925	-0.33289	C14	0.257896	0.452841	H25	0.246328	0.263693
C4	-0.2052	-0.2251	C15	-0.62154	-0.92501	H26	0.376622	0.436774
C5	-0.29024	-0.28431	C16	0.444072	0.626458	H27	0.155427	0.195935
C6	-0.20042	-0.1444	N17	-0.06869	-0.19936	H28	0.172144	0.174771
N7	-0.30832	-0.40677	C18	-0.51572	-0.56395	H29	0.174599	0.177689
S8	0.696897	1.237782	C19	-0.51605	-0.46502	H30	0.153572	0.159892
O9	-0.15653	-0.20566	H20	0.236836	0.274852	H31	0.155571	0.160055
O10	-0.15479	-0.28761	H21	0.161262	0.203053	H32	0.185094	0.189611
N11	-0.4751	-0.8505	H22	0.167124	0.212024	H33	0.167169	0.172159

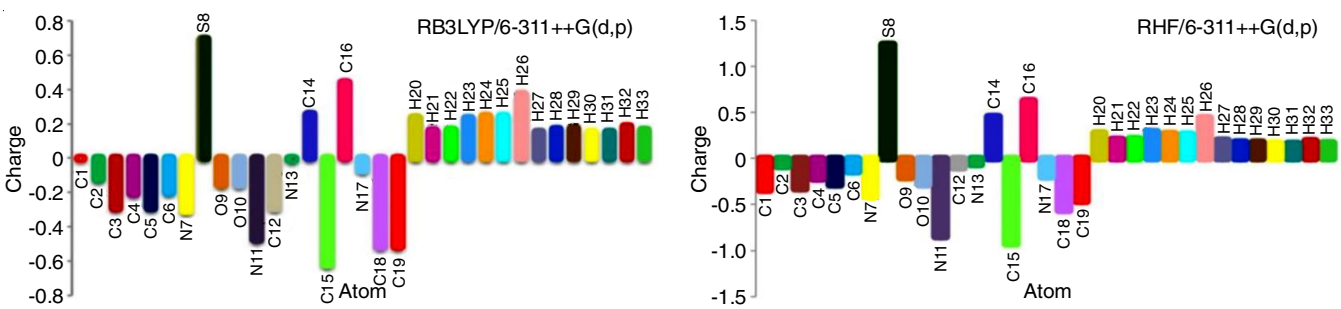

Fig. 6. Mulliken atomic charge distributions of title compound by DFT/RB3LYP and RHF with 6-311++G(d, p) levels in the gas phase

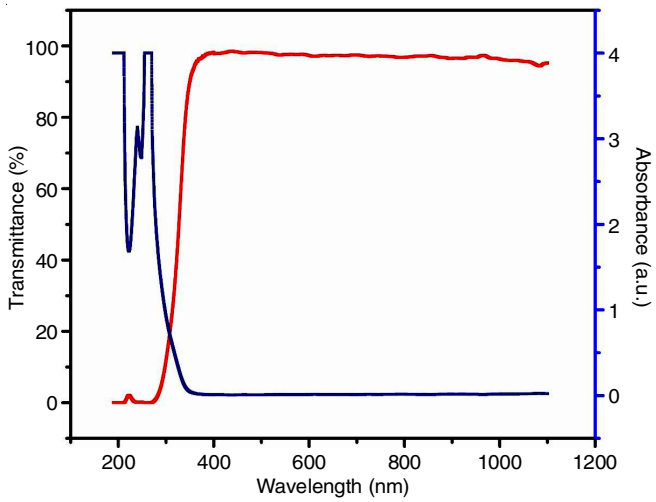

Fig. 7. UV-visible transmittance and absorption spectra of grown single crystal

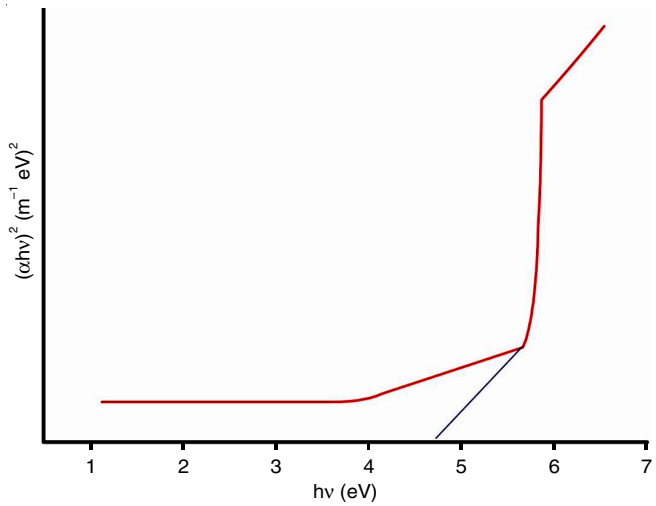

Fig. 8. Plot of photon energy *versus* $(\alpha h\nu)^2$ of the sulfamethazine crystal

Thermal studies: Thermal behaviour of the grown single crystal of sulfamethazine was confirmed by thermogravimetric (TG) and differential thermal analyses (DTA) methods. By application of thermal analysis techniques like thermal gravimetric analysis (TGA), changes in the chemical and physical characteristics of drugs were measured as a function of temperature, ranging from 30 to 689 ºC. Fig. 9 represents the results of TG/DTA investigation on single crystal. The weight loss curve observed in the thermogravimetric analysis (TGA) indicates that the material remains stable up to 210.07 ºC. This indicates that the sulfamethazine crystal had great thermal stability. The process of losing weight has an end reference temperature of 689.05 ºC. The DTA curve's sharp exothermic peak, which was measured at 186 ºC and the TG curve's weight loss coincide. In DTA curve, around 192.14 ºC is the first endothermic peak identified in DTA, which indicates the melting point of the grown crystal. The good crystalline quality of the grown crystal and phase purity are revealed by the sharp endothermic peak that was observed in the DTA spectrum at 254.91 ºC. The lack of any structural changes in the grown sulfamethazine crystal was indicated by the absence of endothermic or exothermic peaks in the temperature range of 30 to 190 ºC.

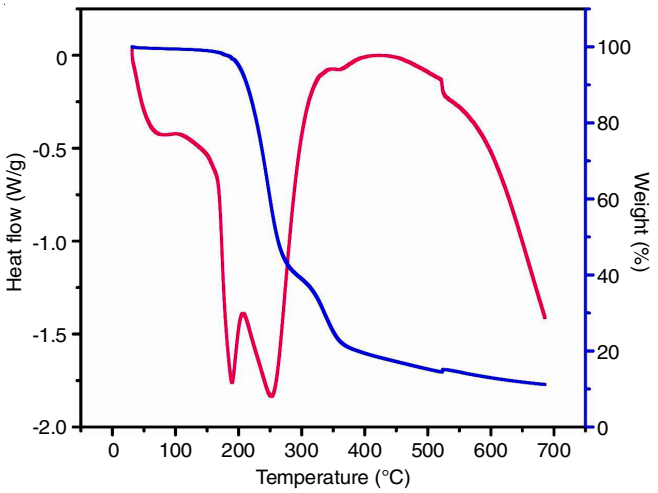

Fig. 9. Thermal analysis of the sulfamethazine single crystal

Antibacterial studies: Using the agar disc diffusion method, pathogenic bacteria were used to determine the *in vitro* antibacterial activity of grown single crystal. According to investigations, sulfamethazine may be more harmful to the growth of Gram-negative *E. coli* bacteria, as shown by a 20 mm zone inhibition. In the grown crystal's antibacterial test, another type of bacteria revealed that Gram-negative bacteria strongly inhibited *S. aureus* with a 20 mm diameter. However, the growth of *E. coli* is inhibited by the presence of grown sulfamethazine crystal, which were used to treat urinary tract infections, while *S. aureus* bacteria were used to treat gastrointestinal diseases.

Conclusion

The sulfamethazine single crystal was successfully grown using slow evaporation technique. The grown crystal belongs to the monoclinic crystal system, according to a single crystal X-ray diffraction (SCXRD) analysis. Density functional theory and Hartree Fock techniques were used to theoretically investigate the optimize geometrical characteristics of sulfamethazine compound. Experimental and theoretical methods were utilized to confirm the functional groups and their vibrational assignments of the grown crystal. A strong correlation has been observed between the calculated and experimental values in the theoretical calculations conducted using the DFT/RB3LYP and RHF methods. Furthermore, the Frontier molecular orbital and Mulliken charge analyses of the molecule were also performed. The UV-Vis spectral analysis was used to examine the transmission percentage, lower cut-off wavelength and optical band gap energy of the grown crystal. The optical band gap of 4.74 eV for a sulfamethazine single crystal suggests potential applications in UV-light-triggered systems, drug delivery or biosensing in pharmaceuticals. The TGA/DTA investigation found that the crystal remains thermally stable up to 210 ºC. The grown crystal has excellent antibacterial properties, making it have applications in the pharmaceutical industry.

ACKNOWLEDGEMENTS

One of the authors, JJB, expresses her gratitude to Manonmaniam Sundaranar University (Registration No. 2021119-2132009) and the Department of Physics and Research Centre

at Sarah Tucker College (Autonomous), Tirunelveli, India, for providing the necessary facilities to carry out this research work.

CONFLICT OF INTEREST

The authors declare that there is no conflict of interests regarding the publication of this article.

REFERENCES

1. A. Ovung and J. Bhattacharyya, *Biophys. Rev.*, **13**, 259 (2021); https://doi.org/10.1007/s12551-021-00795-9
2. T. Ana, N. Vesna, N. Ljubiša and S. Ivan, *Adv. Technol.*, **6**, 58 (2017); https://doi.org/10.5937/savteh1701058T
3. F. de Zayas-Blanco, M.S. García-Falcón and J. Simal-Gándara, *Food Control*, **15**, 375 (2004); https://doi.org/10.1016/S0956-7135(03)00100-2
4. A.K. Basak, S.K. Mazumdar and S. Chaudhuri, *Acta Crystallogr. C*, **39**, 492 (1983); https://doi.org/10.1107/S0108270183005247
5. R.K. Tiwari, M. Haridas and T.P. Singh, *Acta Crystallogr. C*, **40**, 655 (1984); https://doi.org/10.1107/S0108270184005229
6. A.L. Bingham, D.S. Hughes, M.B. Hursthouse, R.W. Lancaster, S. Tavener and T.L. Threlfall, *Chem. Commun.*, 603 (2001); https://doi.org/10.1039/b009540k
7. D.A. Adsmond and D.J. Grant, *J. Pharm. Sci.*, **90**, 2058 (2001); https://doi.org/10.1002/jps.1157
8. S.S. Yang and J.K. Guillory, *J. Pharm. Sci.*, **61**, 26 (1972); https://doi.org/10.1002/jps.2600610104
9. U.H. Patel and K.P. Purohit, *Acta Crystallogr. C Struct. Chem.*, **73**, 9 (2017); https://doi.org/10.1107/S2053229616015898
10. L. Maury, J. Rambaud, B. Pauvert, Y. Lasserre, G. Bergé and M. Audran, *J. Pharm. Sci.*, **74**, 422 (1985); https://doi.org/10.1002/jps.2600740411
11. A.K. Basak, S.K. Mazumdar and S. Chaudhuri, *Acta Crystallogr. C*, **39**, 492 (1983); https://doi.org/10.1107/S0108270183005247
12. Y. Hamada, M. Ono, M. Ohara and E. Yonemochi, *Int. J. Pharm.*, **515**, 416 (2016); https://doi.org/10.1016/j.ijpharm.2016.09.069
13. M. Malagoli and J.L. Brédas, *Chem. Phys. Lett.*, **327**, 13 (2000); https://doi.org/10.1016/S0009-2614(00)00757-0
14. T. van Mourik, M. Bühl and M.-P. Gaigeot, *Philos. Trans.- Royal Soc., Math. Phys. Eng. Sci.*, **372**, 20120488 (2011); https://doi.org/10.1098/rsta.2012.0488
15. S. Muthu and E.I. Paulraj, *Solid State Sci.*, **14**, 476 (2012); https://doi.org/10.1016/j.solidstatesciences.2012.01.028
16. D.R. Delgado and F. Martínez, *Phys. Chem. Liq.*, **53**, 293 (2015); https://doi.org/10.1080/00319104.2014.961191
17. G. Ogruc-Ildiz, S. Akyuz and A.E. Ozel, *J. Mol. Struct.*, **924**, 514 (2009); https://doi.org/10.1016/j.molstruc.2008.12.067
18. N. Elangovan, R. Thomas, S. Sowrirajan and A. Irfan, *J. Indian Chem. Soc.*, **98**, 100144 (2021); https://doi.org/10.1016/j.jics.2021.100144
19. T. Abbaz, A. Bendjeddou and D. Villemin, *ISOR J. Appl. Chem.*, **12**, 60 (2019).
20. F.A. Saad, M.G. Elghalban, N.M. ElMetwaly, H. ElGhamry and A.M. Khedr, *Appl. Organomet. Chem.*, **31**, e3721 (2017); https://doi.org/10.1002/aoc.3721
21. A.M. Mansour, *J. Coord. Chem.*, **66**, 1118 (2013); https://doi.org/10.1080/00958972.2013.775427
22. X. Zheng, S. Chen, L. Gao, Y. Liu, F. Shen and H. Liu, *Environ. Sci. Pollut. Res. Int.*, **27**, 40504 (2020); https://doi.org/10.1007/s11356-020-10072-z
23. Bruker, APEX2 and SAINT, Bruker AXS Inc., Madison, Wisconsin, USA (2009).
24. C. Lee, W. Yang and R.G. Parr, *Phys. Rev. B Condens. Matter*, **37**, 785 (1988); https://doi.org/10.1103/PhysRevB.37.785
25. M.J. Frisch, G.W. Trucks, H.B. Schlegel, G.E.Scuseria, M.A. Robb, J.R. Cheeseman, J.A. Montgomery, T.Vreven, K.N. Kudin, J.C. Burant, J.M. Millam, S.S. Iyengar, J. Tomasi, V. Barone, B. Mennucci, M. Cossi, G. Scalmani, N. Rega, G.A. Petersson, H. Nakatsuji, M. Hada, M. Ehara, K. Toyota, R. Fukuda, J. Hasegawa, M. Ishida, T. Nakajima, Y. Honda, O. Kitao, H. Nakai, M. Klene, X. Li, J.E. Knox, H.P. Hratchian, J.B. Cross, C. Adamo, J. Jaramillo, R. Gomperts, R.E. Stratmann, O. Yazyev, A.J. Austin, R. Cammi, C. Pomelli, J.W. Ochterski, P.Y. Ayala, K. Morokuma, G.A. Voth, P. Salvador, J.J. Dannenberg, V.G. Zakrzewski, S. Dapprich, A.D. Daniels, M.C. Strain, O. Farkas, D.K. Malick, A.D. Rabuck, K. Raghavachari, J.B. Foresman, J.V. Ortiz, Q. Cui, A.G. Baboul, S. Clifford, J.Cioslowski, B.B. Stefanov, G. Liu, A.Liashenko, P. Piskorz, I. Komaromi, R.L. Martin, D.J. Fox, T. Keith, M.A. Al-Laham, C.Y. Peng, A. Nanayakkara, M. Challacombe, P.M.W. Gill, B. Johnson,W. Chen, M.W. Wong, C. Gonzalez and J.A. Pople, Gaussian 03, Revision C.02, Gaussian, Inc., Wallingford CT (2004).
26. N.P. Singh and R.A. Yadav, *Indian J. Phys.*, **75**, 347 (2001).
27. A. Chandran, Y.S. Mary, H.T. Varghese, C.Y. Panicker, P. Pazdera and G. Rajendran, *Spectrochim. Acta A Mol. Biomol. Spectrosc.*, **79**, 1584 (2011); https://doi.org/10.1016/j.saa.2011.05.015
28. V.K. Rastogi, M.A. Palafox, R.P. Tanwar and L. Mittal, *Spectrochim. Acta A Mol. Biomol. Spectrosc.*, **58**, 1987 (2002); https://doi.org/10.1016/S1386-1425(01)00650-3
29. G. Thilagavathi and M. Arivazhagan, *Spectrochim. Acta A Mol. Biomol. Spectrosc.*, **79**, 389 (2011); https://doi.org/10.1016/j.saa.2011.01.052
30. R. Anitha, S. Athimoolam and M. Gunasekaran, *Spectrochim. Acta A Mol. Biomol. Spectrosc.*, **138**, 753 (2015); https://doi.org/10.1016/j.saa.2014.11.077
31. M. Boopathi, P. Udhayakala, T.V. Rajendiran and S. Gunasekaran, *J. Appl. Spectrosc.*, **83**, 12 (2016); https://doi.org/10.1007/s10812-016-0235-z
32. N.P. Roeges and J.M.A. Baas, A Guide to the Complete Interpretation of Infrared Spectra of Organic Structures, New York: Wiley, p. 122 (1994).
33. M. Govindarajan, K. Ganasan, S. Periandy and S. Mohan, *Spectrochim. Acta A Mol. Biomol. Spectrosc.*, **76**, 12 (2010); https://doi.org/10.1016/j.saa.2010.02.029
34. G. Socrates, Infrared and Raman Characteristic Group Frequencies: Tables and Charts, John Wiley & Sons (2004).
35. R.M. Silverstein and G.C. Bassler, *J. Chem. Educ.*, **39**, 546 (1962); https://doi.org/10.1021/ed039p546
36. S. Gorog, Ultraviolet-Visible Spectrophotometry in Pharmaceutical Analysis, CRC Press (2018).